# Supplementary Information

## Supplementary 1 - Energy, net moment and toroid moment

The magnetic energy $U$ can be scaled with

$$U_0 = \frac{\mu_0 m_0^2}{4\pi d^3} \,,$$

where $d$ is a characteristic lengthscale (e.g. the edge length of the cube), $m_0$ a dipole moment scale and $\mu_0$ the vacuum permeability. The dimensionless energy $E$ per dipole can then be defined as

$$E = \frac{U}{N U_0} = \frac{1}{N} \sum_{i<j}^{N} \frac{\mathbf{m}_i \cdot \mathbf{m}_j - 3 \left( \mathbf{m}_i \cdot \mathbf{e}_{ij} \right) \left( \mathbf{m}_j \cdot \mathbf{e}_{ij} \right)}{|\mathbf{r}_{ij}|^3} \,, \tag{1}$$

where $\mathbf{m}_1, .., \mathbf{m}_N$ describe the dimensionless moments of the $N$ freely orientable dipoles of equal magnitude $|\mathbf{m}_i| = 1$ and $\mathbf{r}_{ij}$ is the dimensionless relative position vector between dipole $i$ and $j$ with $\mathbf{e}_{ij}$ denoting the corresponding unit vector.

The net magnetic moment is defined as

$$\mathbf{M} = \frac{1}{N} \sum_{i=1}^{N} \mathbf{m}_i \,,$$

which is a discrete analogue to the magnetization. The normalization of the moments $|\mathbf{m}_i| = 1$ guarantees that $|\mathbf{M}| \leq 1$. The toroid moment is defined with respect to a given point $c$ in space as

$$\mathbf{T} = \frac{1}{N} \sum_{i=1}^{N} \mathbf{p}_i \times \mathbf{m}_i \,,$$

1

where $\mathbf{p}_i$ is the vector from the point $c$ to the position of dipole $i$, see e.g. [1]. The magnetic dipole moment $\mathbf{m}$ can be thought of as a current loop in the limit where its area $A$ goes to zero while its current $I$ diverges, keeping the product $|\mathbf{m}| = AI$ constant. In the same sense, the toroid moment $\mathbf{T}$ can be envisioned as a toroidal inductor coil in the limit where the torus radius $R$ and cross-sectional tube area $A$ go to zero while the current $I$ diverges, keeping the product $|\mathbf{T}| = RAI$ constant. $\mathbf{T}$ is useful to describe vortex-like states of dipole configurations, like e.g. planar head-to-tail ring configurations, for which $|\mathbf{T}|$ is maximal. For the cube continuum we have $\mathbf{M} = 0$ and $\mathbf{T} = 0$ with respect to the center of the cube.

## Supplementary 2 - System of equilibrium equations

Finding all equilibria of a dynamical system with energy $E$ is equivalent to finding all states of the system where the gradient vanishes. In general, the gradient has as many components as there are degrees of freedom in the system, in our case $2N$: Two angles per dipole to describe its orientation. However, we found that the use of cartesian coordinates to describe the dipole orientations is advantageous compared to the angle formulation: Firstly, we avoid the inherent coordinate singularities of spherical coordinates. Secondly, the degree of the resulting system of polynomial equations is lower (quadratic instead of quartic). Thirdly, the structure of the equations is highly symmetric.

Let the orientation of dipole $i$ be given as $\mathbf{m}_i = (x_i, y_i, z_i)^\mathsf{T}$, then we can

define the full orientation vector

$$\boldsymbol{\Omega} := \left(x_1, y_1, z_1, ..., x_N, y_N, z_N\right)^\mathsf{T},$$

which contains the orientations of all dipoles. The energy $E$ can now be written as a symmetric bilinear form $E(\boldsymbol{\Omega}, \boldsymbol{\Omega})$ with the representation

$$E = \frac{1}{2}\boldsymbol{\Omega}^\mathsf{T}\mathbf{W}\,\boldsymbol{\Omega} \qquad \text{or} \qquad E = \frac{1}{2}\sum_{i,j=1}^{3N}\Omega^i\,W_i^j\,\Omega_j\,,$$

where $\mathbf{W}$ is the symmetric $3N \times 3N$ interaction matrix which encodes the positional information of all dipoles. $\mathbf{W}$ is constant for a given arrangement (like e.g. the cube). With the definition of the linear combinations

$$L_{ik} := \sum_{j=1}^{3N} W_{3(i-1)+k}^j\,\Omega_j\,, \qquad i = 1, 2, ..., N\,, \qquad k = 1, 2, 3\,,$$

the zero gradient equations (i.e. equilibrium conditions) for all dipoles can be expressed in the form of the $3N$ cyclic equations

$$
\begin{aligned}
L_{i1}\,y_i &= L_{i2}\,x_i \\
L_{i2}\,z_i &= L_{i3}\,y_i \qquad\qquad i = 1, 2, ..., N \qquad\qquad (2)\\
L_{i3}\,x_i &= L_{i1}\,z_i\,.
\end{aligned}
$$

Since we assume fixed magnitudes for the moments $|\mathbf{m}_i| = 1$ the cartesian description demands $N$ additional "sphere" equations

$$x_i^2 + y_i^2 + z_i^2 = 1\,, \qquad i = 1, 2, ..., N\,. \tag{3}$$

Altogether Eqs. (2) and (3) set up a strongly coupled system of $4N$ quadratic polynomial equations in the $3N$ unknown components of $\boldsymbol{\Omega}$.

## Supplementary 3 - Upper bound for the number of isolated equilibria

To get an upper bound for the number of possible isolated solutions, our overdetermined system Eqs. (2) and (3) with $4N$ equations for $3N$ unknowns has to be reformulated. We "randomize down" to a square system: The system is replaced by $3N$ random linear combinations of the original $4N$ equations, cf. [2]. Then, a variant of Bertini's theorem (see e.g. [3] p.163) assures that the set of isolated solutions for the randomized system is a superset of the original system. Therefore, every upper bound (for the number of isolated solutions) for the randomized system is one for the original system as well.

Now we use the basic version of Bézout's theorem: A polynomial system with $n$ variables and $n$ equations of total degree $d_1, .., d_n$ has at most $S_{\mathsf{max}} := d_1 d_2 ... d_n$ isolated solutions. The randomized system with $3N$ variables consists of $3N$ quadratic polynomial equations (i.e. the total degree is always 2). Therefore we have $S_{\mathsf{max}} = 2^{3N}$ possible isolated solutions, which is also an upper bound for the original system (see above). Compared to the analogous analysis for the angle formulation ($S_{\mathsf{max}} = 2^{6N}$) this is a significantly better bound.

## Supplementary 4 - Numerical solution method

The system of polynomial Eqs. (2) and (3) is solved with the open-source software Bertini™: Software for Numerical Algebraic Geometry [4]. This nu-

merical software framework is developed for industrial problems including mechanism and robot kinematics, chemistry, and computer-aided design, to name a few. However, it can be used to solve any system of polynomial equations. The manageable system sizes for numerical programs like Bertini™ are much greater compared to symbolic manipulation programs which utilize Gröbner bases and related methods, see e.g. [5].

The numerical algorithm in Bertini™ is based on homotopy continuation and uses modern methods like randomization techniques and regenerative cascades, see [6, 3]. The general idea of homotopy continuation in order to solve a system $\Sigma$, is to consider another system $\Sigma^\star$ with known solutions and deform $\Sigma^\star$ to $\Sigma$. The deformation is achieved through a parameterization of the system equations, such that they reduce to $\Sigma$ and $\Sigma^\star$ for different parameter values.

A parallel version of the software is available based on the Message Passing Interface (MPI). An overview of the theoretical background in algebraic geometry, a detailed description of the numerical algorithm and a comprehensive user manual for Bertini™ can be found in book [3].

The software provides information about the number of solution components and their dimensions. Further, for 0D (isolated) components it gives the numerical values of the solutions up to any required precision. For higher dimensional components any number of sampling points can be generated.

## Supplementary 5 - Stability

We now prove the formula connecting the trace of the Hessian matrix $\mathbf{H}$ (the sum of all eigenvalues $\lambda_k$) with the magnetic energy $E$

$$\sum_{k=1}^{2N} \lambda_k = \mathsf{Tr}\,(\mathbf{H}) = -4E. \tag{4}$$

Here it is convenient to use spherical coordinates with the polar and azimuthal angles $\theta_i$ and $\phi_i$ to describe the orientation of dipole $i$

$$\mathbf{m}_i = \begin{pmatrix} x_i \\ y_i \\ z_i \end{pmatrix} = \begin{pmatrix} \cos\phi_i \sin\theta_i \\ \sin\phi_i \sin\theta_i \\ \cos\theta_i \end{pmatrix}. \tag{5}$$

The energy $E$ in Eq. (1) consists of sums of component-wise products of the dipole moments. If we define $\epsilon_i$ to collect all terms of $E$ containing $\theta_i$ and $\phi_i$ we can write with Eq. (5)

$$\epsilon_i := A_i \cos\phi_i \sin\theta_i + B_i \sin\phi_i \sin\theta_i + C_i \cos\theta_i \,, \tag{6}$$

where $A_i, B_i, C_i$ depend on all other angles but not on $\theta_i$ and $\phi_i$. Note that since all terms of $E$ consist of pairs of different moments, every term appears in two different $\epsilon_i$ and we have

$$E = \frac{1}{2} \sum_{i=1}^{N} \epsilon_i \,. \tag{7}$$

We need the $2N$ diagonal entries of $\mathbf{H}$, which are the second covariant derivatives of $E$ with respect to all angles $\theta_1, \phi_1, \theta_2, \phi_2, ..., \theta_N, \phi_N$. We may replace $E$ with the respective $\epsilon_i$ when differentiating with respect to $\theta_i$ and $\phi_i$ and

get the diagonal entries

$$H_{11} = \frac{\partial^2 \epsilon_1}{\partial \theta_1^2}, \qquad H_{22} = \frac{1}{\sin^2 \theta_1} \frac{\partial^2 \epsilon_1}{\partial \phi_1^2} + \cot \frac{\partial \epsilon_1}{\partial \theta_1},$$

$$H_{33} = \frac{\partial^2 \epsilon_2}{\partial \theta_2^2}, \qquad H_{44} = \frac{1}{\sin^2 \theta_2} \frac{\partial^2 \epsilon_2}{\partial \phi_2^2} + \cot \frac{\partial \epsilon_2}{\partial \theta_2}, \qquad (8)$$

$$\vdots \qquad\qquad \vdots$$

The extra "cot . . ." term when differentiating with respect to $\phi$ is a direct result of the second covariant derivative in spherical coordinates. Inserting Eq. (6) into (8) we find

$$H_{11} = H_{22} = -\epsilon_1, \qquad H_{33} = H_{44} = -\epsilon_2, \qquad \ldots$$

and therefore

$$\mathsf{Tr}\,(\mathbf{H}) = \sum_{k=1}^{2N} H_{kk} = -2 \sum_{i=1}^{N} \epsilon_i.$$

This together with Eq. (7) proves relation (4). Note that the only condition on $E$ for Eq. (4) to hold is that $E$ consists only of component-wise products of two moments. There may be other types of interactions to which this relation is applicable.

## Supplementary 6 - Robustness of the continuous ground state

To demonstrate the existence of the continuous ground state as well as the robustness and practicability of the magnetic coupling, we actually designed and built two different constructions of the cubic dipole cluster, see Figure 1. In both experiments the theoretical finding that the ground state continuum
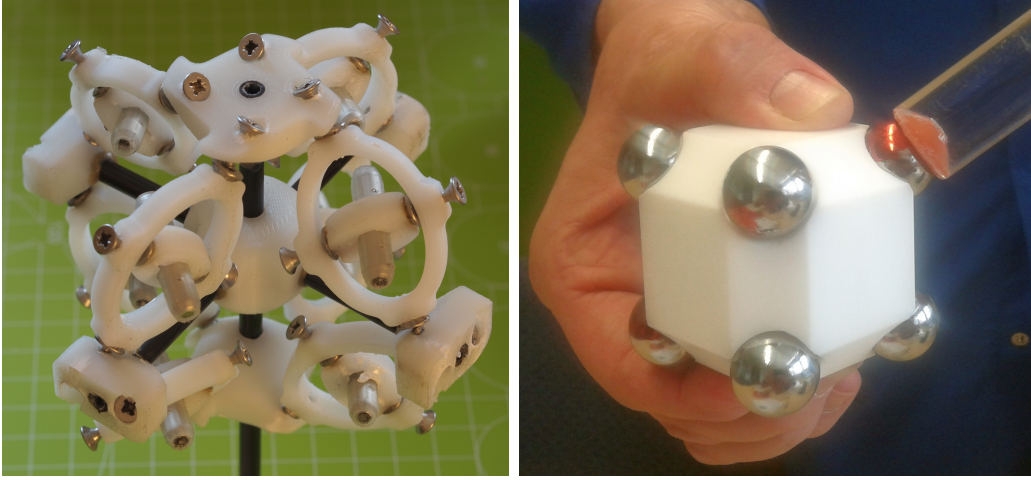
7

Figure 1: Practical realizations of the cubic dipole cluster. **Left:** A construction which allows 8 Geomag™ toy magnets to rotate freely in their gimbal-mounts. All white parts are produced with a 3D printer, the black rods are made of carbon fiber and the bearings are realized with non-magnetic screws. The centerpoints of the dipoles form a cube with an edge length of exactly 40 mm, see [7]. **Right:** A Teflon™ block with holes drilled in the corners, allowing 8 spherical magnets to glide easily and therefore rotate freely. The resulting magnetic forces are attractive and automatically fix the spheres in the corners (i.e. the spheres are attracted towards the center). With a color mark on the spheres (in red) one can see the motion of all spheres along the continuum if one rotates one of them around its respective space diagonal (done here with a glass tube with a rubber end).

is the only stable state is confirmed: Any other initial states relaxes immediately back to the ground state. The motion along the continuum is smooth with no noticeable force variations already for these first two prototype constructions.

To quantify the influence of possible imperfections in the construction of the magnetic coupling, we perform an analysis of the continuum for a perturbed system. For that we displace one of the dipoles in a random di-
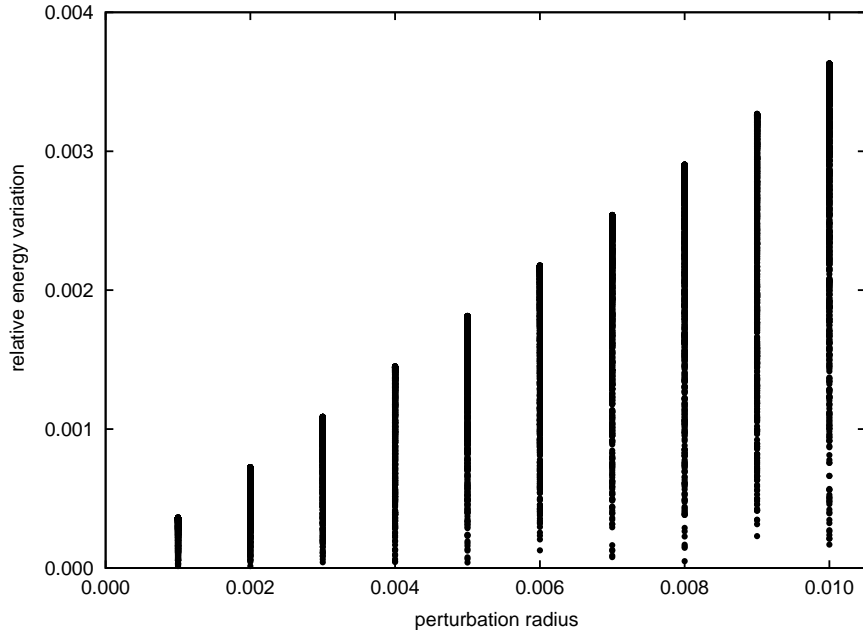
Figure 2: Smoothness of the appearing soft mode for the perturbed system characterized by the relative energy variation. The variation is shown as a function of the perturbation radius by which one dipole is displaced in a random direction. The radius is given relative to the cube's edge length. For each radius, 1000 random directions are computed. The largest variation of about 0.37% (for a radius of 1%) occurs for displacement directions perpendicular to the rotation axis, i.e. the space diagonal of the cube. For directions along the rotation axis the variations are smallest. The upper limit for the variation depends linearly on the perturbation radius.

rection with a given perturbation radius away from its original position. In the considered range for the perturbation radius (it does not exceed 1% of the cube's edge length) the perturbed ground state remains the only stable configuration. Still the system can not jump to a different stable equilibrium. The former continuum becomes a soft mode in the perturbed state. The important quantity characterizing how flat this soft mode will be, is the relative

energy variation, given as: The magnitude of the sinusoidal-like magnetic energy variation along the mode divided by the mode's mean magnetic energy. The dependence of the relative energy variation on the perturbation radius is shown in Figure 2. The maximum variation depends linearly on the perturbation radius, showing that no catastrophic alterations in the dynamics occur, the system is structurally stable.

# References

[1] Melenev, P, Rusakov, V, & Raikher, Y. (2006) *Journal of Magnetism and Magnetic Materials* **300**, e187 – e190.

[2] Sommese, A. J & Verschelde, J. (2000) *Journal of Complexity* **16**, 572 – 602.

[3] Bates, D. J, Hauenstein, J. D, Sommese, A. J, & Wampler, C. W. (2013) *Numerically solving polynomial systems with Bertini.* (SIAM).

[4] (2014) (https://bertini.nd.edu/).

[5] Decker, W, Greuel, G.-M, Pfister, G, & Schönemann, H. (2012) Singular 3-1-6 — A computer algebra system for polynomial computations (http://www.singular.uni-kl.de).

[6] Hauenstein, J. D, Sommese, A. J, & Wampler, C. W. (2011) *Applied Mathematics and Computation* **218**, 1240 – 1246.

[7] Grunwald, M. (2014) (http://audiots.wordpress.com/).